EFFECT OF OXYGEN ORDERING

ON BULK AND THIN FILM CERAMIC SUPERCONDUCTORS

Y. Bruynseraede, J. Vanacken, B. Wuyts, C.-M. Fu,
Q. Xu, C. Van Haesendonck, and I.K. Schuller*

Laboratorium voor Vaste Stof-Fysika en Magnetisme
Katholieke Universiteit Leuven
3030 Leuven, Belgium
* Physics Department - B019
University of California - San Diego
La Jolla, CA 92093, USA.

Abstract

It is now well established that the physical properties of high T_c oxide compounds are very sensitive to the oxygen ordering and stoichiometry. Changes in the oxygen content can induce structural transformations, metal-insulator transitions, variations in the transition temperature, and may influence the critical current and field properties. A review will be given of the oxygen kinetics in $YBa_2Cu_3O_x$ and the effect of oxygen deficiency and vacancy ordering on the superconducting properties of bulk and thin film ceramic superconductors.

Proceedings, TMS Symposium on "High Temperature Superconducting Compounds", Anaheim, 1990.

1. Introduction

Oxygen doping in the high-T_c copper-oxides is one of the crucial parameters for the occurrence of superconductivity in these materials [1]. Changes in the oxygen content induce structural transformations, metal-insulator transitions, and variations in the onset temperature for magnetic and superconducting order. From oxygen and rare-earth or transition metal doping [2], it is possible to determine which parameters of these perovskite structures are important for understanding the origin of the superconductivity. It is now well established that the valence (or oxidation state) of $[Cu\text{-}O]^{+x}$ is influenced by the uptake or removal of oxygen. One could assume that the formal valence of Cu is greater than two for the p-type materials, and less than two for the n-type. On the other hand, measurements of the x-ray absorption [3] and electron spectroscopy [4,5] seem to indicate that extra holes do not change the valence of the Cu from +2, but instead lie on the oxygen. The local structural order also influences the superconductivity [6] either due to a substitution in the CuO_2 planes, or due to a change in bond length, affecting a transfer of charge in these CuO_2 planes [1,7].

Soon after the discovery [8] of the 90 K superconductivity, the lattice structure of $YBa_2Cu_3O_x$ was determined by x-ray and neutron diffraction [9]. The structural phase transition (orthorhombic to tetragonal) was found to be driven by the oxygen content [10], while the oxygen vacancy distribution in the planes and/or chains is related to the appearance of superconductivity [11,12]. Most research on the effect of oxygen stoichiometry has been performed in the $YBa_2Cu_3O_x$ system, because of the presence of loosely bound and easily removable oxygen in the Cu-O chains.

When studying the oxygen kinetics in high-T_c copper-oxides, it is necessary to consider the oxidation reaction as well as the oxygen diffusion processes [13,14]. Using oxygen evolution techniques it is possible to identify different desorption mechanisms and to detect impurity phases [15-18]. Detailed information about the oxygen stoichiometry in thin films is difficult or impossible to obtain from neutron diffraction, thermogravimetry or chemical methods. Raman scattering [19] and eventually sensitive oxygen evolution experiments are able to determine the oxygen stoichiometry in thin film systems.

The general structure of this paper is as follows. In section 2, we consider in detail the oxygen kinetics in $YBa_2Cu_3O_x$. In section 3, we discuss oxygen diffusion in bulk and thin film systems. Finally, in section 4, the effect of the oxygen stoichiometry on the critical temperature and the perovskite structure are analysed.

2. Oxygen Kinetics

It has already been shown extensively that $YBa_2Cu_3O_x$ and related compounds exist for a wide range of oxygen stoichiometry [1]. The physical properties depend not only on the amount of oxygen in the material, but also on its location in the lattice. Neutron diffraction studies showed clear evidence that oxygen can easily be lost from the chains (O1 sites), due to the weak binding energy [9,10,22]. As the oxygen content is reduced, T_c decreases until the system becomes finally semiconducting. This oxygen which is lost, can again be replaced to reproduce the original superconducting material [20,21].

Oxygen ordering in $YBa_2Cu_3O_x$ is also responsible for the tetragonal to orthorhombic phase transition at high temperature and can produce additional superstructures at low temperature [23,24,25]. It has recently been suggested [26] that such ordered superstructures are closely related to the existence of "plateaus" in the T_c versus oxygen concentration curve, as observed by various investigators [18,27,28,29].

Due to the oxygen ordering effects, the exact oxygen content x at the orthorhombic to tetragonal phase transition depends on the sample preparation technique : some authors report a value of 6.6 for samples prepared by quenching from high temperatures [30], while others have observed an orthorhombic structure down to $x = 6.3$ for samples prepared by a Zr gettering technique at low temperature [31].

Since the oxygen stoichiometry strongly influences the superconducting properties, an exact knowledge of the oxygen kinetics in these materials is extremely important. From

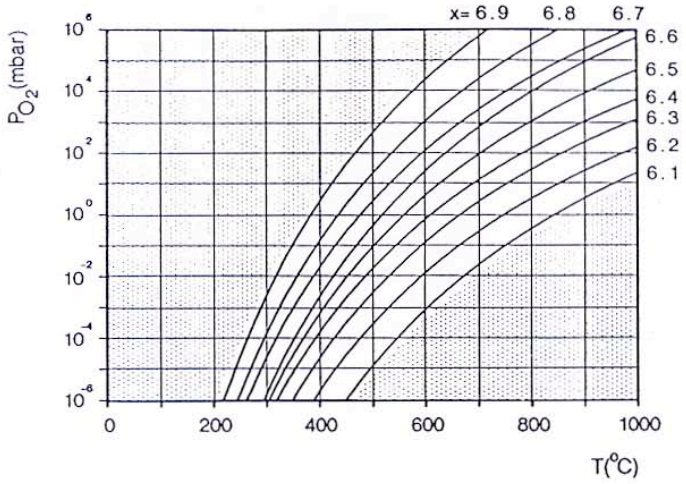

Figure 1 - *P-T diagram, derived from [30], indicating for each temperature the oxygen partial pressure for which $YBa_2Cu_3O_x$ is stable (solid lines for different x values). The dotted regions on the left ($x > 6.9$) and the right side ($x < 6.1$) indicate instability regions.*

a thermodynamical point of view, it is clear that the oxygen content of the perovskite structure is determined by the temperture T of the system, and the environmental oxygen partial pressure P_{O_2} [29]. P_{O_2}-T diagrams have been reported by several authors and were determined by thermogravimetry in different oxygen flows [30] or by electromotive force measurements [32,33]. Figure 1 shows the P_{O_2}-T diagram of $YBa_2Cu_3O_x$ for several x values. The diagram was calculated from the results of Gallagher (solid lines) which were extrapolated to lower pressures. These diagrams indicate for each temperature the corresponding oxygen partial pressure at which the oxygen deficient compound is stable. The $x = 6.1$ and $x = 6.9$ curves in the P_{O_2}-T diagram delimit a region of thermodynamic stability for $YBa_2Cu_3O_x$. Outside this region, the compound will contain secondary phases [33,34]. These instability regions in the diagram are very important for the *in situ* fabrication of thin films : the formation of unwanted secondary phases can be avoided by the right choice of substrate temperature and oxygen partial pressure.

We have studied the oxygen kinetics using a gas evolution technique [18]. In this method, we heat (10°C/min to $\sim$ 900°C) a small sample (typically 10 mg) placed in an evacuated quartz tube . During the heating procedure, the pressure in the tube is monitored using a very sensitive capacitance manometer or a quadrupole mass spectrometer. The elevated heating rate implies that the oxygen desorption is dominated by diffusion. In order to rule out spurious effects due to the evolution of impurity gases, the evolved gas is analyzed using the mass spectrometer. The data are corrected for measured changes observed in the empty tube due to gas evolution from the walls of the vessel. Knowing the tube volume and the sample mass, one can easily calculate the average amount of oxygen atoms per unit cell, x, released by the sample.

Figure 2 shows oxygen evolution curves for several bulk superconducting ceramics, with or without Cu-O chains. The various peaks is the evolution curve of $YBa_2Cu_3O_x$ clearly indicate that different oxygen desorption processes occur at specific temperatures. The spectrum for the $YBa_2Cu_3O_x$ compound is in good agreement with the spectra obtained by Miura et al. [35] using a temperature programmed desorption method, and with the spectra obtained by Biswas et al. [36] using thermogravimetry.

The oxygen kinetics in the compounds containing Cu-O linear chains ($YBa_2Cu_3O_7$, $LaBa_2Cu_3O_7$, $Y_{1-x}Pr_xBa_2Cu_3O_7$) already start at $T \simeq 400$°C, while in the other materials they start at much higher temperatures. The broad peak at around 600°C seems to exhibit a shoulder, hiding a second broad peak. These two peaks could be assigned to ordered (O1 site) and disordered (O1/O5 sites) oxygen atoms respectively, in agreement with Miura

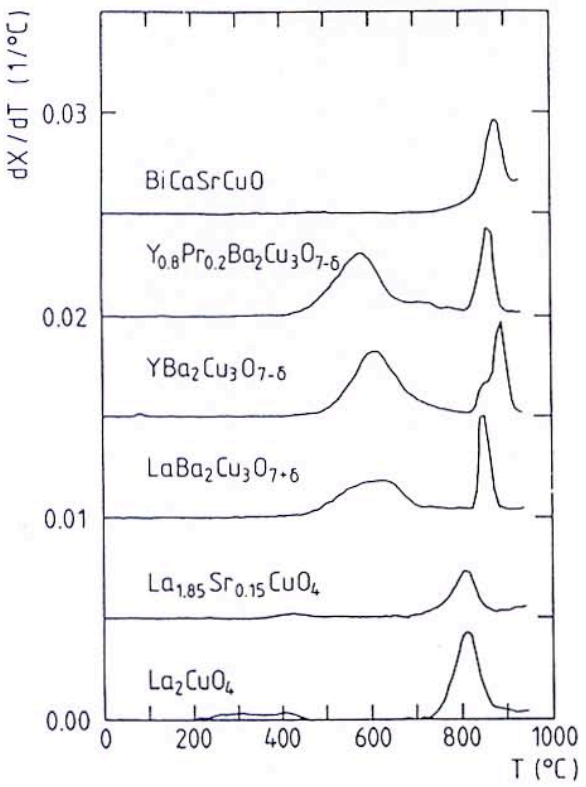

Figure 2 - *Oxygen evolution curves for different ceramic oxides with or without Cu-O chains. The curves are shifted upwards for clarity.*

et al. [35], and confirmed by neutron diffraction [9]. Indeed, the pressure in the tube being of the order of 1 mbar at this stage of the heating, the orthorhombic - tetragonal phase transition occurs at T $\simeq$ 600°C, as can be derived from the P_{O_2}-T diagram (Fig. 1), assuming that the transition takes place when x $\simeq$ 6.5 $\pm$0.05.

All the samples in Fig. 2 exhibit one or more desorption peaks at higher temperatures (T > 800°C), as also observed by Miura et al. and Biswas et al. We assume [37] that these peaks can be attributed to impurity phases present in the sample together with a decomposition of the material. Indeed, looking again to the P_{O_2}-T diagram in Fig. 1, and in particular to the critical region reported by Bormann et al., the decomposition area starts at T $\simeq$ 800°C for $P_{O_2} \simeq$ 1 mbar.

It is possible to describe the oxygen evolution curves theoretically using a single site desorption relation [17], providing the activation energies and frequency factors for the observed processes. In this way, we found activation energies ΔE $\simeq$ 1.2 eV for the first peak and ΔE $\simeq$ 2.8 eV for the high temperature peaks. However, one must be careful in interpreting these activation energies, since they reflect a combination of three different processes occur : (i) a hopping process of an oxygen atom to the grain boundary via vacant sites; (ii) a diffusion process through the grain boundaries towards the sample surface; (iii) a desorption process to escape from the surface.

To conclude this section, we would like to illustrate the sensitivity of the gas evolution technique with a curve for the "electron" high-T_c compound $Nd_{1.85}Ce_{0.15}CuO_4$ (see Fig. 3). For this compound we recorded the signal of molecular oxygen during heating, using a mass spectrometer. We observed two regions of oxygen out-diffusion : one around 350°C (see insert) and one above 700°C, in agreement with the results of Wang et al. [38]. However, the amount of oxygen contained in the low temperature part is much smaller than in the high temperature part. Wang et al. assigned the low temperature signal to disordered oxygen in interstitial sites (with their presence depending on the sample history), and the increase at high temperatures to ordered oxygen atoms arising from the same sites. In our experiments, we did not observe any influence of the sample

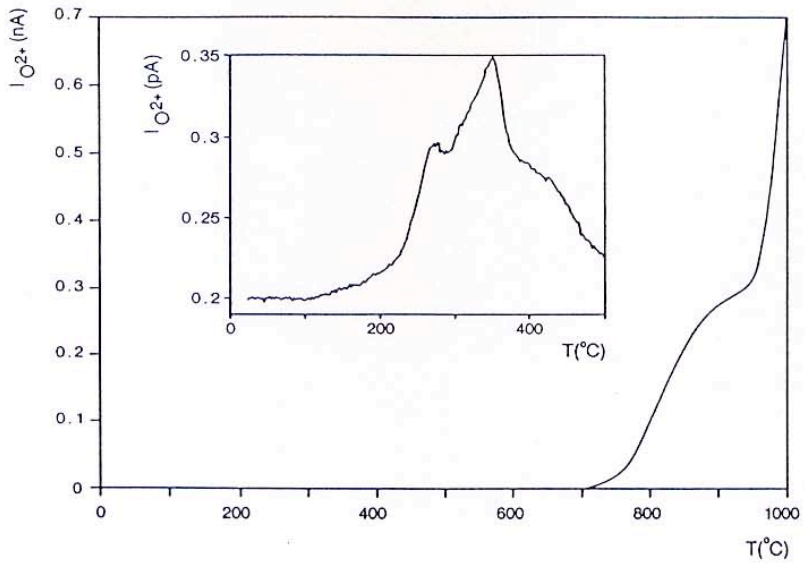

Figure 3 - *Oxygen evolution curve for* $Nd_{2-x}Ce_xCuO_4$. *The compound looses oxygen at* $T \sim 450°C$ *(see enlarged signal in insert) and for* $T > 750°C$.

history (in particular the cooling rate) on the appearance of the 350°C peak. Moreover, we did not notice any correlation of this peak with the superconducting properties. To induce superconductivity in the compound, it is necessary to reduce the oxygen content at temperatures higher than 750°C, as reported by Wang et al. [38].

3. Oxygen Diffusion

A detailed understanding of the oxygen diffusion process in the ceramic is not only important for material processing, but it also provides us with unique information on the dynamics of oxygen vacancies and their interaction with the environment [39]. Using these data, the oxygen ordering phase di gram as a function of temperature and pressure can be calculated (see for example de Fontaine [40]).

Although the oxygen diffusivity and solubility within the bulk perovskite structure are important kinetic parameters, the oxygen mobility is also strongly influenced by boundary conditions. More specifically, this mobility depends on the grain size, preferred orientation of grains, intergranular cracking, density and porosity, and the presence of surface and grain boundary phases. All these parameters are crucial for the adsorption and desorption of the oxygen at the surface of the material [41] and hence limit the rate of out- and in-diffusion from the sample.

As an example, Fig. 4 shows respectively the desorption spectra for a single crystal ($\sim 2 \times 1 \times 1$ mm^3) (lower curve), a polycrystalline pellet ($\sim$ 2mg) (middle) and a thin film ($\sim 4 \times 4 \times 10^{-3}$ mm^3) (upper) of $YBa_2Cu_3O_x$, obtained using the gas evolution technique described in the previous section. The broad peak corresponding to the oxygen evolution from the Cu-O chains shifts towards lower temperatures for the pellet and the thin film. As mentioned in the previous section, we can assign an effective activation energy to this broad peak. The larger the grain size, the larger the activation energy for out-diffusion will be. Resistivity measurements have also indicated that the activation energy for the oxygen diffusion out from a powder sample is lower than that for a sintered pellet [42]. These experiments also revealed the important role played by the surface potential barrier in the mechanism of the out- diffusion. By coating the grains of a polycrystalline $YBa_2Cu_3O_x$ sample with Ag, one can reduce this surface potential barrier [43].

Plasma oxidation allows to considerably reduce the effective energy activation barrier for oxygen diffusion. Greene and Bagley [2] showed that after plasma oxidation, a non-superconducting $YBa_2Cu_3O_x$ sample of size $0.5 \times 5 \times 12$ mm^3 can have a Meissner effect up to 24% after a 285 hr treatment. On the other hand, the complete oxidation of a thin film takes only a few minutes. The plasma oxidation enhances the reactivity of the oxygen, thus lowering the surface barrier. The plasma oxidation technique is very promising for thin film microelectronic device applications since it enables to control the oxidation of $YBa_2Cu_3O_x$ at lower temperature ($\sim$ 100°C) [45,44], with small thermo-induced disorder. Moreover, it can be performed at low power density avoiding the degradation of the material properties.

For most of the diffusion measurements, one observes that the oxygen diffusivity can be described by an Arrhenius behavior i.e. the diffusion is thermally actived. Although the diffusion problem is extremely complex for superconducting ceramics, the results have been interpreted in terms of a single (isotropic) effective diffusion coefficient [46,47,48]. The importance of the correlation among moving oxygen atoms was pointed out by Bakker [49]. In his model, similar to atomic diffusion in order-disorder metallic compounds, the diffusion coefficient depends on the degree of disorder which governs the efficiency of the atomic jumping for long distance migration. A more useful model should treat the correlated hopping (or tunneling) process in a highly anisotropic self-consistent potential.

We will now discuss in detail the different experimental techniques used to determine the effective activation energy ΔE and the oxygen diffusion coefficient D. Table 1 summarizes the experimental ΔE and D values reported in the literature. Most efforts have been concentrated on $YBa_2Cu_3O_x$ because of the reversible "oxygen sponge" properties of this compound.

The most common method is a weight measurement performed in the **dynamical** (fixed heating rate) or **isothermal** (as a function of time) mode. This **thermogravimetric analysis (TGA)** can be performed in the presence or absence of oxygen, in order to determine the in-diffusion or out-diffusion constants respectively [42,50,51]. A similar technique is **Differential Scanning Calorimetry (DSC)** [52].

An alternative method for the TGA is the oxygen desorption technique described in section 2. Figure 5 shows the desorption results for various heating rates in $YBa_2Cu_3O_x$. As shown in the insert, the peaks in the desorption spectra shift towards higher temperature with increasing heating rate, in agreement with the fact that a faster heating rate implies a shorter time available for diffusion at a given temperature.

In situ resistivity measurements as a function of the temperature have been extensively used by Tu et al. [41,53,54,55]. In contrast to the TGA method, the calculated activation energies are smaller. This is probably due to the fact that the resistivity is determined by a percolation mechanism and is therefore more sensitive to the oxygen stoichiometry of the surface, than to the bulk diffusion properties.

The oxygen diffusion can also be explored by using a **solid-state electrochemical cell** with an yttria-stabilized zirconnia (YSZ) single crystal wafer serving as the electrolyte [56]. On one side of the YSZ, two electrodes of sputtered Au films are deposited, while the ceramic pellet of $YBa_2Cu_3O_x$ is pressed against the other side of the YSZ. Using this setup, oxygen can be driven in and out of the $YBa_2Cu_3O_x$ electrode under controlled conditions. This method gives identical results for the in- and the out-diffusion processes.

The diffusion processes can also be investigated by **polarized light microscopy**. This method is based on the direct observation of the oxygen diffusion front separating the tetragonal from the orthorhombic phase, under different annealing conditions [57]. Again, this method cannot distinguish between the in- and the out-diffusion processes, because the motion of O-T domain wall does not reflect the details of the oxygen diffusion process.

In contrast to the above methods, the **oxygen tracer measurement** can be used to derive the diffusion coefficient in the absence of a chemical gradient [39]. It is important to note that the the tracer diffusion is different from the chemical diffusion. The current theoretical models cannot explain the observed phenomena quantitatively.

Finally, the **internal friction (IF)** as a function of temperature was measured at $\sim$ 1 Hz in an automatic inverted torsional pendulum by Xie et al. [60]. They pointed out that the IF is induced by the stress relaxation of individual oxygen atoms in the random walk diffusion process.

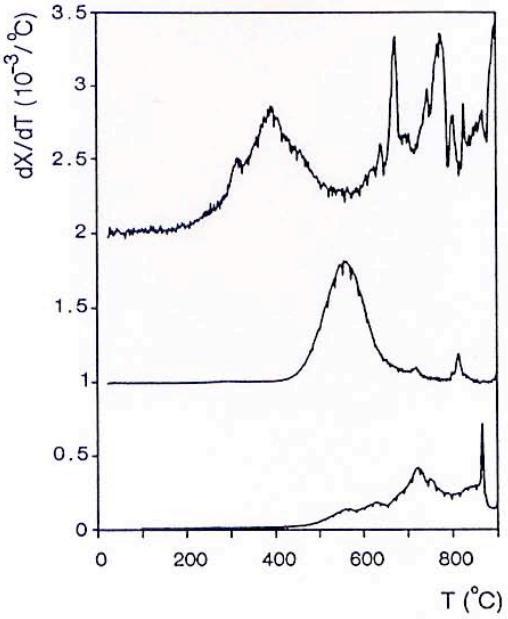

Figure 4 - *Oxygen evolution curves (shifted upwards for clarity) for $YBa_2Cu_3O_x$: the upper curve represents the result for a thin film ($\sim 4 \times 4 \times 0.001\ mm^3$), the middle curve is for a sintered pellet ($\sim 2\ mg$) and the lower for a single crystal ($\sim 2 \times 1 \times 1\ mm^3$).*

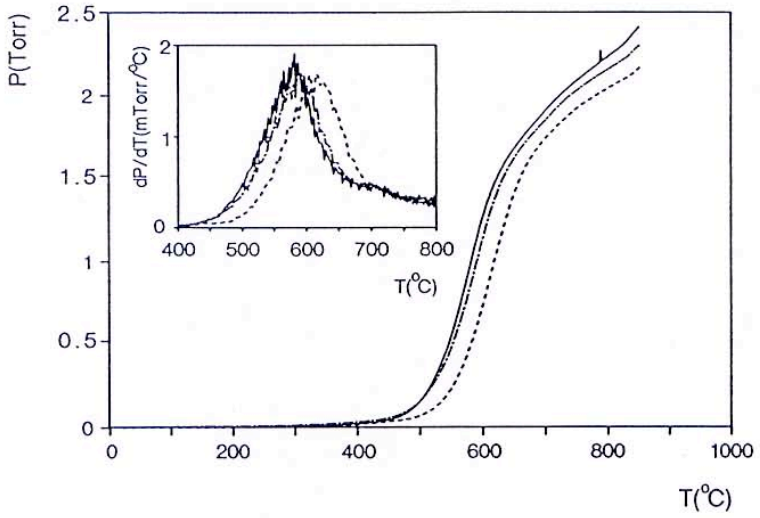

Figure 5 - *Oxygen evolution curves (oxygen pressure P versus T; insert shows the derivative signal) for an $YBa_2Cu_3O_x$ sample, repeatedly desorbed with different heating rates : 8 °C/min for the solid line, 11 °C/min for the dashed line and 15 °C/min for the dotted line.*

Table 1 - Diffusion constant and activation energies in $YBa_2Cu_3O_x$ (dynamical method (d), isothermal method (i), in-diffusion (id), and out-diffusion (od)).

Experiment	ΔE * (eV)	D (cm^2s^{-1})	Remarks **	Ref.
weight loss (TGA)	1.52	-	(d)	[42]
	1.25	-	powder , (d)	[42]
	1.2	$10^{-6} - 10^{-7}$ (500 °C)		[50]
	0.26 ($x \simeq 6.5$)	9×10^{-12} (500 °C)	powder , (i)	[51]
DSC	1.5-1.6	$7 - 50 \times 10^{-12}$ (400 °C)	powder $\sim 2\mu m$ (d)	[52]
Resistivity	1.1	-	(id, i)	[53]
	0.48 ($x = 6.6$)	-	(id, i)	[53]
	1.7	-	(od, i)	[54]
	0.5 ($x = 6.6$)	-	(id, d)	[41]
	1.3	2×10^{-11}	(id, d)	[41]
	1.7	-	(od, d)	[41]
solid-state electrochem.	-	5×10^{-8} (550 °C)	(i)	[56]
	1.5	2×10^{-7} (500 °C)	(i)	[58]
polarized light	0.38	3.4×10^{-6} (500 °C)		[57]
tracer O^{18}	0.89	1.4×10^{-11} (500 °C)	thermodynami-	[39]
	0.99	8×10^{-12} (527 °C)	cal equilibrium	[59]
internal friction	1.25	1.7×10^{-12} (500 °C)		[60]
gas evolution	1.2	-	(d)	[17]

* Fully oxygenated samples except when indicated otherwise.

** All data have been obtained on sintered pellets except when indicated otherwise.

In conclusion, the oxygen diffusion process in the superconducting ceramic $YBa_2Cu_3O_x$ is very complex. Even when the simple picture of Fick is used, the diffusion dynamics depend strongly on the boundary and initial conditions. Up to now, only effective potential barriers have been introduced to describe the diffusion coefficients. It is generally accepted that the activation energy for oxygen diffusion in $YBa_2Cu_3O_x$ in the tetragonal phase is smaller than in the orthorhombic phase (see Table 1). However, one needs more detailed analysis of the experimental results to determine the influence of parameters such as sample geometry , sample homogeneity, etc. Different experimental techniques probe different physical properties during/after the oxygen diffusion, and therefore they will reveal different aspects of the oxygen diffusion mechanism. More elaborated microscopic models are needed to take into account the full details of the oxygen diffusion mechanism.

The oxygen diffusion at the sample surface is a very important problem. It is of industrial interest to find optimal catalytic conditions in order to improve the material processing.

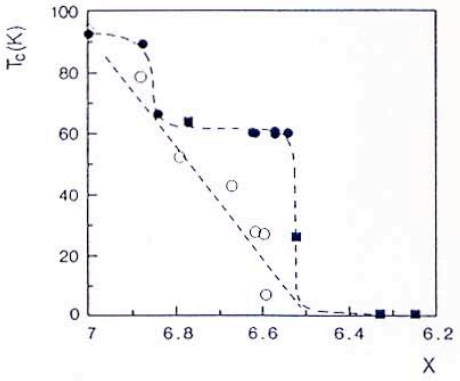

Figure 6 - *Mid-point critical temperature versus oxygen content x in $YBa_2Cu_3O_x$ (from [62]). Open symbols = resistively determined for samples quenched from high temperatures; closed symbols = for slowly annealed (low T) samples (circles = resistively determined, squares = inductively determined).*

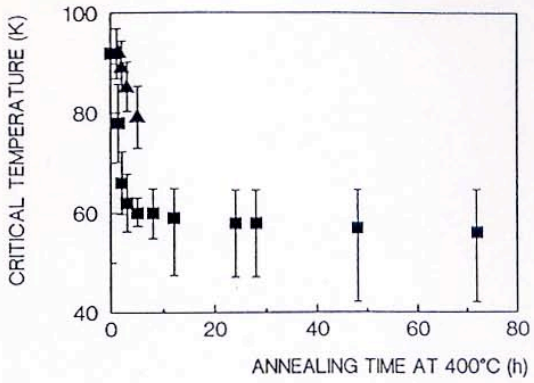

Figure 7 - *Critical temperature versus annealing time at 400 °C. For short annealing times, two distinct superconducting phases were observed (square + triangle). The error-bars denote the transition width.*

4. Influence of the oxygen content on the superconducting properties

As indicated in the previous sections, the oxygen content can be modified in a reversible way in $YBa_2Cu_3O_x$. This also implies that the superconducting transition temperature can be tuned continuously by adapting the oxygen content.

Many experiments have focused on the exact shape of the T_c versus oxygen content (x) curve, which is strongly affected by the material preparation conditions. In general, one can conclude that the T_c(x) curve shows a plateau around 60 K when the the oxygen is gently removed via out-diffusion at lower temperatures (T $\sim$ 400 °C) [27,28,29,37]. On the other hand, a more monotoneous reduction of T_c (plateau is less pronounced or completely absent) is observed when the oxygen is removed more abruptly by quenching the samples from more elevated temperatures [61,62]. A typical example for the two types of behavior is shown in Fig. 6 (from [62]). T_c is defined as the mid-point of the main superconducting transition. For the quenched samples (open circles), the T_c values were obtained from the resistive transition. For the slowly annealled samples, T_c was determined from resistive measurements (full circles) as well as from the Meissner effect (full squares).

In order to clearly define the superconducting properties of a given sample, one should always combine the results of resistive as well as inductive measurements. The resistive transition will be determined by the infinite cluster having the highest transition temperature. For all experiments, the oxygen content x corresponds to an average over the complete sample. Locally, a higher oxygen content may induce a finite T_c value, while the larger part of the sample is already insulating. On the other hand, the inductive measurements of T_c directly reflect the relative importance of the various phases having a different T_c. Using our previously introduced desorption setup (section 2), we were able to prepare oxygen deficient samples by vacuum annealing at T $\simeq$ 400 °C and P $\simeq 10^{-6}$ mbar, for which we have measured the superconducting poperties inductively. Figure 7 shows the observed T_c depression as a function of the annealing time [37]. Using the

oxygen evolution results, it is possible to translate the annealing time into an oxygen loss from the Cu-O chains (600 °C peak in Fig. 2). We find that the oxygen content decreases from $x \simeq 6.9$ towards $x \simeq 6.4$ when the annealing time increases. It is important to note that most of this oxygen is lost during the first 20 hours of the vacuum annealing process. Between 20 hours and 100 hours, the oxygen content remains basically constant.

Our own rf susceptibilty measurements [37] reveal that, while the T_c value is close to 60 K for annealing times between 10 hours and 100 hours (see Fig. 7), the relative importance of the 60 K Meissner fraction is strongly reduced with increasing annealing time. This indicates that the oxygen deficient samples have an highly inhomogeneous distribution of the oxygen atoms, resulting in important spatial variations of the superconducting order. Since the total oxygen content does not change, one has to assume that a different ordering of the oxygen vacancies on the O1 and O5 site, is responsible for the observed behavior. Intuitively, one expects that this different arrangement of the oxygen vacancies can also explain the width of the 60 K plateau as well as the exact x value at which the orthorhombic to tetragonal phase transition is occurring.

Starting from Transmission Electron Microscopy (TEM) studies, several attempts have been made to show that the appearance of the 60K phase is caused by the formation of a periodic lattice where due to the oxygen deficiency, only every other chain is occupied by oxygen atoms ($2a_o$ super-structure) [24,25,63,64]. The interpretation of these results remains still controversial since TEM pictures can only be made at the edge of the samples or in regions which have been thinned (and damaged ?) via ion bombardment. TEM studies will mainly image regions which are very likely to be more oxygen deficient than the starting bulk material. It is therefore very difficult to link the observed superconducting properties for the bulk material to the different lattice structures which are observed in the TEM studies. In any case, the TEM pictures confirm that the oxygen desorption is highly inhomogeneous, implying the coexistence of several oxygen super-structures within the same sample. Neutron diffraction experiments can not provide useful information since they always sample a large volume containing the different phases. The neutron data will only reflect the average orthorhombic distortion and cannot distinguish between different oxygen super-structures.

Acknowledgements

We would like to thank I. Mangelschots (IBM - Zürich) for providing us with $Nd_{2-x}Ce_xCuO_4$ samples. This work is supported by the Belgian F.K.F.O., the I.U.A.P. and G.O.A. Programs (at K.U.L.) and the U.S. National Science Foundation under grant No. 8803185 (at U.C.S.D.). International travel was provided by a NATO grant. J.V. is a Research Fellow of the Belgian I.W.O.N.L., B.W. is a Research Fellow of the Belgian F.K.F.O. and C.V.H. is a Research Associate of the Belgian N.F.W.O.

References

[1] For a review, see J.-M. Tarascon and B.G. Bagley, MRS Bulletin **14**, 53 (1989); Proc. of Conference on Oxygen Disorder Effects in High-T_c Superconductors, Trieste (Italy), April 1989 (to be published).

[2] For a review, see L.H. Greene and B.G. Bagley, in "Physical Properties of High Temperature Superconductors II", D.M. Ginsberg, ed. (World Scientific Press, Singapore, 1990) (to be published).

[3] J.M. Tranquada, S.M. Heald, A.R. Moodenbaugh, and M. Suenaga, Phys. Rev. B**35**, 7187 (1987); J.M. Tranquada, S.M. Heald, and A.R. Moodenbaugh, Phys. Rev. B**36**, 5263 (1987).

[4] C.N.R. Rao, P. Ganguly, M.S. Hegde, and D.D. Sharma, J. Amer. Chem. Soc. **109**, 6893 (1987).

[5] N. Nücker, J. Fink, J.C. Fuggle, P.J. Durhamand, and W.M. Temmerman, Phys. Rev. B**37**, 5158 (1988).

[6] L.H. Greene, J.-M. Tarascon, B.G. Bagley, P. Barboux, W.R. McKinnon, and G.W. Hull, Rev. Solid State Science **1**, 199 (1987).

[7] R.J. Cava, B. Batlogg, S.A. Sunshine, T. Siegrist, R.M. Fleming, K. Rabe, L.F. Schneemeyer, D.W. Murphy, R.B. Van Dover, P.K. Gallagher, S.H. Glarum, S. Nakahara, R.C. Farrow, J.J. Krajewski, S.M. Zahurak, J.V. Waszczak, J.H. Marshall, P. Marsh, L.W. Rupp, Jr., W.F. Peck, and E.A. Rietmann, Physica C **153-155**, 560 (1988).

[8] M.K. Wu, J.R. Ashburn, C.J. Torng, P.H. Hor, R.L. Meng, L. Gao, Z.J. Huang, Y.Q. Wang, and C.W. Chu, Phys. Rev. Lett. **58**, 908 (1987).

[9] For a review of the relevant literature, see J.D. Jorgensen, Jpn. J. Appl. Phys. **26** (supplement 26-3), 2017 (1987).

[10] J.D. Jorgensen, M.A. Beno, D.G. Hinks, L. Soderholm, K.J. Volin, R.L. Hitterman, J.D. Grace, Ivan K. Schuller, C.U. Segre, K. Zhang, and M.S. Kleefisch, Phys. Rev. B**36**, 3608 (1987).

[11] I.K. Schuller, D.G. Hinks, M.A. Beno, D.W. Capone II, L. Soderholm, J.-P. Locquet, Y. Bruynseraede, C.U. Segre, and K. Zhang, Solid State Commun. **63**, 385 (1987).

[12] C.U. Segre, B. Dabrowski, D.G. Hinks, K. Zhang, J.D. Jorgensen, M.A. Beno, and I.K. Schuller, Nature **329**, 227 (1987).

[13] H. Verweij, Ann. Phys. Fr. **13**, 349 (1988).

[14] H. Bakker, J.P.A. Westerveld, D.M.R. Lo Cascio, and D.O. Welch, Physica C **157**, 25 (1989).

[15] H. Strauven, J.-P. Locquet, O.B. Verbeke, and Y. Bruynseraede, Solid State Commun. **65**, 293 (1988).

[16] J.-P. Locquet, H. Strauven, B. Wuyts, O.B. Verbeke, K. Zhang, I.K. Schuller, J. Vanacken, C. Van Haesendonck, and Y. Bruynseraede, Physica C **153-155**, 822 (1988).

[17] J.-P. Locquet, J. Vanacken, B. Wuyts, Y. Bruynseraede, K. Zhang, and I.K. Schuller, Europhys. Lett. **7**, 469 (1988).

[18] J.-P. Locquet, J. Vanacken, B. Wuyts, Y. Bruynseraede, and I.K. Schuller, Europhys. Lett. **10**, 365 (1989).

[19] K.Y. Yang, H. Homma, R. Lee, R. Bhadra, M. Grimsditch, S.D. Bader, J.-P. Locquet, Y. Bruynseraede, and I.K Schuller, Appl. Phys. Lett. **53**, 808 (1988).

[20] J.-M. Tarascon, W.R. McKinnon, L.H. Greene, G.W. Hull, and E.M. Vogel, Phys. Rev. B**36**, 226 (1987).

[21] P.K. Gallagher, H.M. O'Bryan, S.A. Sunshine, and D.W. Murphy, Mater. Res. Bull. **22**, 995 (1987).

[22] J.E. Greedan, A. O'Reilly, and C.V. Stager, Phys. Rev. B**35**, 8770 (1987).

[23] R. Beyers and T. Shaw, in "Solid State Physics, Advances in Research and Applications", H. Ehrenreich and D. Turnbull, eds., 135-212 (Academic Press, New York, 1989).

[24] J. Reyes-Gasga, T. Krekels, G. Van Tendeloo, J. Van Landuyt, S. Amelinckx, W.H.M. Bruggink, and H. Verweij, Physica C **159**, 831 (1989).

[25] R. Beyers, B.T. Ahn, G. Gorman, V.Y. Lee, S.S.P. Parkin, M.L. Raminez, K.P. Roche, J.E. Vazquez, T.M. Gür, and R.A. Huggins, Nature **340**, 619 (1989).

[26] D. de Fontaine, G. Ceder, and M. Asta, Nature (to be published).

[27] R.J. Cava, B. Batlogg, C.H. Chen, E.A. Rietman, S.M. Zahurak, and D. Werder, Nature **329**, 423 (1987).

[28] J.M. Tranquada, D.E. Cox, W. Kunnmann, H. Moudden, G. Shirane, M. Suenaga, P. Zolliker, D. Vaknin, S.K. Sinha, M.S. Alvarez, A.J. Jacobson, and D.C. Johnston, Phys. Rev. Lett. **60**, 156 (1988).

[29] J.D. Jorgensen, H. Shaked, D.G. Hinks, B. Dabrowski, B.W. Veal, A.P. Paulikas, L.J. Nowicki, G.W. Crabtree, W.K. Kwok, L.H. Nunez, and H. Claus, Physica C **153-155**, 578 (1988).

[30] P.K. Gallagher, Advanced Ceramic Materials **2**, 632 (1987).

[31] R.J. Cava, B. Batlogg, C.H. Chen, E.A. Rietman, S.M. Zahurak, and D. Werder, Phys. Rev. B**36**, 5719 (1987).

[32] M. Tetenbaum, L.A. Curtiss, B. Tani, B. Czech, and M. Blander, Proc. of NATO Advanced Study Institute on High Temperature Superconductors - Physics and Materials Science, Bad Windsheim (Germany), August 13-26, 1989 (to be published).

[33] R. Bormann and J. Nölting, Appl. Phys. Lett. **54**, 2148 (1989); R. Bormann and J. Nölting, Physica C **162-164**, 81 (1989).

[34] D.E. Morris, J.H. Nickel, J.Y.T. Wei, N.G. Asmar, J.S. Scott, U.M. Scheven, C.T. Hultgren, A.G. Markelz, J.E. Post, P.J. Heaney, D.R. Veblen, and R.M. Hazen, Phys. Rev. B**39**, 7347 (1989).

[35] N. Miura, H. Suzuta, Y. Teraoka, and N. Yamazoe, Jpn. J. Appl. Phys. **27**, L337 (1988).

[36] P. Biswas, D. Zhou, J. Grothaus, P. Boolchand, and D. McDaniel, Proc. of the MRS Symposium M (1990) (to be published).

[37] B. Wuyts, J. Vanacken, J.-P. Locquet, C. Van Haesendonck, Ivan K. Schuller, and Y. Bruynseraede, Proc. of NATO Advanced Study Institute on High Temperature Superconductors - Physics and Materials Science, Bad Windsheim (Germany), August 13-26, 1989 (to be published).

[38] E. Wang, J.-M. Tarascon, L.H. Greene, G.W. Hull, and W.R. McKinnon, Phys. Rev. B (to be published).

[39] S.J. Rothman, J.L. Routbort, L.J. Nowicki, K.C. Goretta, L.J. Thompson, J.N. Mundy, and J.E. Baker, Proc. of DIMETA-88, International Conference on diffusion in Metals and Alloys, Balatonfured (Hungary), September 5-9, 1988.

[40] D. de Fontaine, Proc. of Conference on "Oxygen Disorder Effects in High T_c Superconductors", J.L. Moran-Lopez, ed., Trieste (Italy), April 1989.

[41] K.N. Tu, N.C. Yeh, S.I. Park, and C.C. Tsuei, Phys. Rev. B**39**, 304 (1989).

[42] L.T. Shi and K.N. Tu, Appl. Phys. Lett. **55**, 1351 (1989).

[43] A.G. Schrott, G. Singco, and K.N. Tu, Appl. Phys. Lett. **55**, 2126 (1989); A.G. Schrott, K.N. Tu, N.C. Yeh, G. Singco, A. Levy, and C.C. Tsuei, Phys. Rev. B**39**, 2910 (1989).